Ceramics-Silikáty 63 (1), 93-99 (2019)
www.ceramics-silikaty.cz doi: 10.13168/cs.2019.0001

PREPARATION OF ZrB_2 BY BORO/CARBOTHERMAL REDUCTION IN SPS DEVICE

CINERT J.*, **, #CTIBOR P.*, BROŽEK V.**, BOUDA V.*, L. MASTNÝ***

*Department of Electrotechnology, Faculty of Electrical Engineering, Czech Technical University, Technicka 2, 166 27 Prague 6, Czech Republic
**Institute of Plasma Physics, ASCR, Za Slovankou 3, 182 00 Prague 8, Czech Republic
***University of Chemistry and Technology, Prague, Czech Republic, Technicka 5, 166 28 Prague 6, Czech Republic

#E-mail: ctibor@ipp.cas.cz

Submitted October 23, 2018; accepted December 19, 2018

Keywords: Zirconium diboride, Zirconia, Boron carbide, Borothermal reaction, Carbothermal reaction, Spark plasma sintering (SPS)

ZrB_2 ceramics were prepared by boro/carbothermal reduction, using spark plasma sintering (SPS). This technology allows to control and monitor the ongoing reduction reaction during the sintering of ZrO_2 and B_4C powder mixtures with graphite, leading to the production of ZrB_2. This work shows the effect of several parameters on the amount of produced ZrB_2. The results are compared with literature data. Sintering temperatures in the range 1400 - 1800 °C were chosen for the experiment. For example, after sintering at a temperature of 1800 °C, with a hold time of 15 min, the total amount of ZrB_2 produced from a powder mixture of stoichiometric ratio was more than 60 %. The porosity dropped with increasing sintering temperature to a final value of about 0.3 %. The number of pore sections per square unit dropped with the temperature as well. The final product is composed of very hard as well as rather soft components.

INTRODUCTION

Borides, e.g. ZrB_2 [1], belong to the group of ultra-high temperature ceramics (UHTCs), together with Hf- and Ta-carbides [2, 3]. ZrB_2 has favorable intrinsic characteristics such as high melting point, high hardness, good chemical inertness and high wear resistance [4], which make it a promising candidate for high-temperature structural applications. Recently, much effort has been devoted to the research of these materials, compared to the very popular and widely used transition metal silicides [5-8]. These UHTCs materials are potential candidates for thermal protection of materials in both re-entry and hypersonic aerospace vehicles [3, 9]. ZrB_2 exhibits a mass gain kinetics that is affected by diffusion-limited processes in the low temperature regime. The upper temperature limit of this regime depends on factors such as external pressure, oxygen partial pressure and gas flow rate, but is generally assumed to be between 1100 and 1200 °C in static air. Increased heat resistance, studied in the papers [4, 10, 11], seems to be caused by using ZrB_2 with a specific concentration of SiC. It has been proven [12] that B_2O_3 begins to evaporate and SiC begins to corrode at temperatures above 1100 °C. Formation of a sub-layer of borosilicate glass on the outside surface of the oxide layer results in a logarithmic time dependence of mass gain [12]. The evaporation of silica at temperatures above 1600 °C leads to a loss of the protection effect of the remaining ZrO_2 layer [13]. Massive oxidation rate, bubble formation and evaporation of silica at temperatures above 2200 °C has been mentioned in earlier work [14]. ZrB_2 can be prepared by boro/carbothermal reaction of ZrO_2 and B_4C with using graphite [15, 16] or bituminous coal in a graphite crucible, heated under argon atmosphere at temperature 1250 °C for one hour. Another way of ZrB_2 preparation by the boro/carbothermal reaction is via the spark plasma sintering (SPS) technique, as shown elsewhere [17, 18]. The preparation of ZrB_2 by using the SPS technique leads to shorter production process times compared with the two techniques mentioned above. This work is focused on the preparation of ZrB_2 ceramics by boro/carbothermal reaction sintering using SPS equipment.

EXPERIMENTAL

Coarse zirconia/ZrO_2 powder (Russia) with a grain size range 25 - 40 μm, B_4C (Tetra, former ČSSR) with a grain size less than 20 μm and even finer graphite powder have been used as raw materials. All powders were mixed in stoichiometric ratio, according to the reaction (1) below, and mechanically blended. The final powder was compacted by the SPS technique (SPS 10-4, Thermal Technology, USA). Sintering temperatures were chosen in temperature range from 1400 °C to 1800 °C, the heating rate was 100 °C·min^{-1} and the pressure increase rate was 10 MPa·min^{-1} up to the final value 70 MPa. All samples were sintered within 15 min after the required sintering temperature was reached. After the 15 min dwell time a cooling rate of 30 °C·min^{-1} was applied. Sintered samples of cylindrical shape were prepared. Their diameter was 19 mm and height 3 mm. The samples were cut and specimens were prepared for microstructural characterization. The microstructure was observed on the polished section using scanning electron microscopy/SEM (EVO MA 15, Carl Zeiss SMT, Germany) in the backscattered electron mode (SEM-BSE). Porosity was determined by image analysis (IA) applied to optical micrographs (with magnification 500×). Also microhardness was determined by optical microscopy, using a Vickers indenter attached to a Hanemann head. The samples were inserted into standard sample holders for X-ray diffraction/XRD analysis by the so-called side loading procedure in order to minimize the occurrence of preferred orientation. These samples were measured in standard Bragg-Brentano geometry with divergent beam and with the beam knife placed above the samples in order to minimize the effects of air scattering. Since our next aim was to measure the centres of the sintered samples, the irradiated volumes were chosen to be in the middle of the samples cross sections. Therefore, a polycapillary and collimator of 1 mm in diameter were inserted into the primary X-ray beam path, changing the originally divergent character into quasi-parallel. Diffracted CuKα radiation was detected by a 1D LynxEye detector. The used X-ray diffactometer (D8 Discover, Bruker, Germany) was equipped with a laser system and a compact *x*, *y*, *z* stage, facilitating precise positioning of the measured surface.

RESULTS AND DISCUSSION

Densification behavior

The prepared mixture of ZrO_2, B_4C and graphite was sintered at temperatures from 1400 °C to 1800 °C (100 °C steps) by the SPS technique. The recorded parameters of the sintering process were: punch position, sintering temperature and pressure, vacuum in the process chamber, sintering time. Two sintering processes (for temperatures 1500 °C and 1800 °C) are shown on Figure 1 and Figure 2.

The most important parameters for the evaluation of the sintering process are the punch displacement (i.e. the distance between the pressing punches) and the change of the vacuum level. These values indicate the degree of compaction of the sintering powder.

The biggest advantage of SPS is the rapid heating rate and the simultaneously applied pressure on the compacted powder. As ZrB_2 has a relatively low electrical resistivity (30-40 μΩ·cm) [1, 2], the samples are heated uniformly. The applied pressure brings the sintered particles closer to each other and creates more contact points, enabling faster diffusion. Both effects (rapid heating rate and pressure) result in very short sintering times compared to other sintering techniques. Therefore a relatively short dwell time of 15 minutes was applied in the present work.

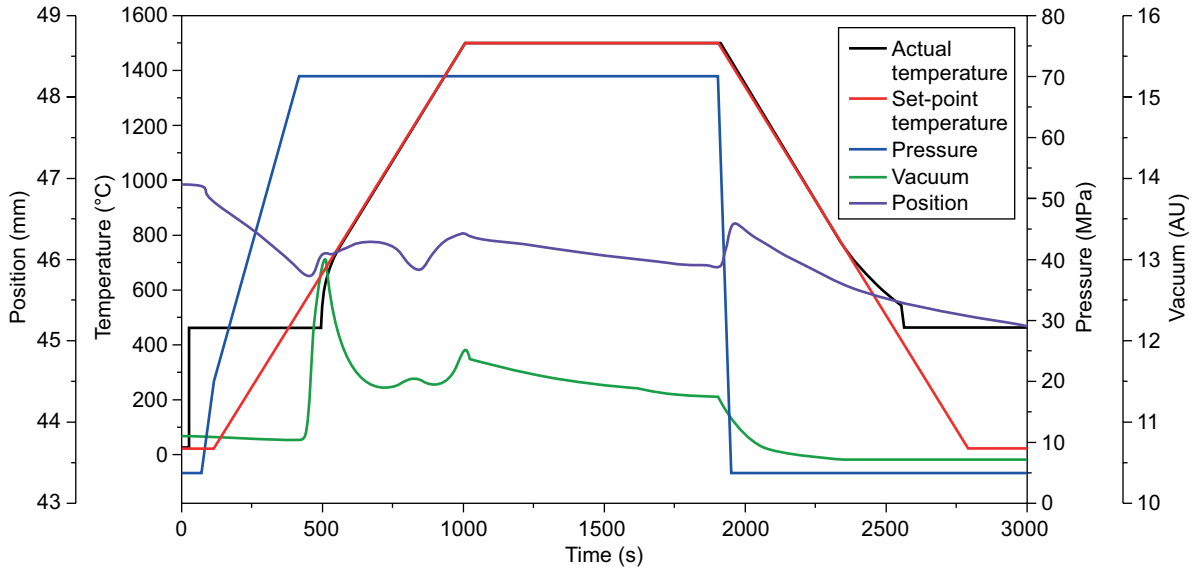

Figure 1. Process parameters during sintering the mixture of ZrO_2, B_4C and graphite powder at 1500 °C.

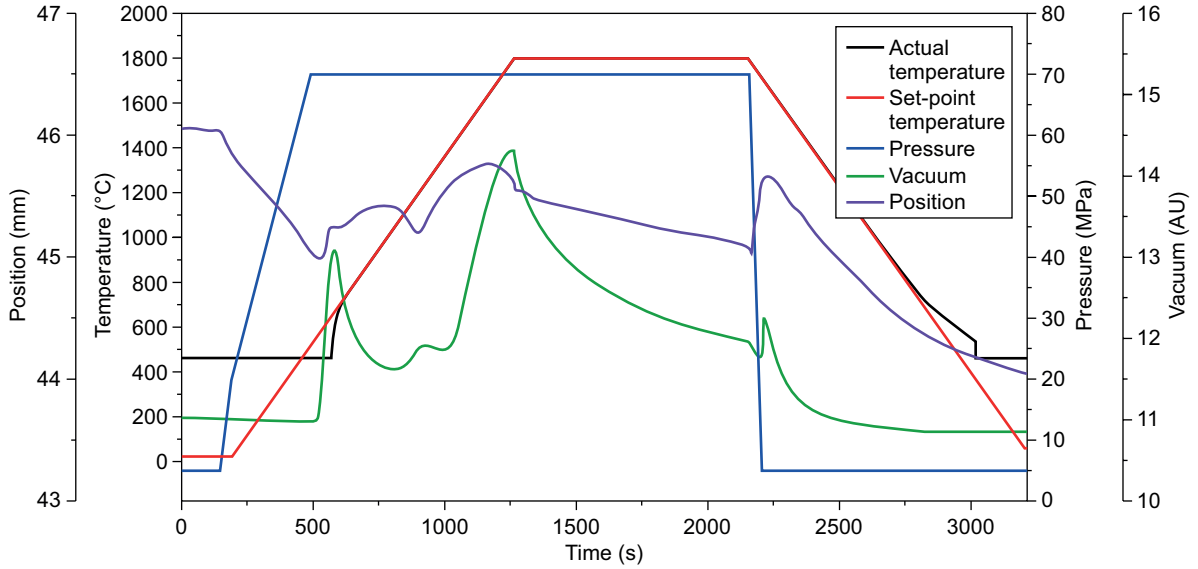

Figure 2. Process parameters during sintering of the mixture of ZrO_2, B_4C and graphite powder at 1800 °C.

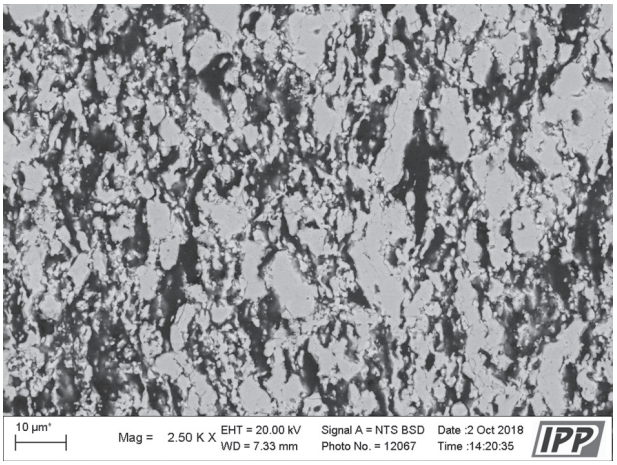

Figure 3. Polished section of sample sintered at 1500 °C for 15 min (SEM-BSE).

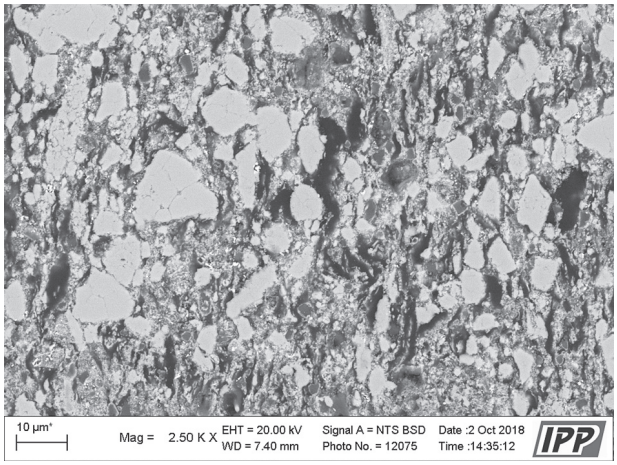

Figure 4. Polished section of sample sintered at 1800 °C for 15 min (SEM-BSE).

Microstructure of polished section

Figures 3 and 4 show microstructures of the sintered samples prepared at temperatures from 1500 °C and 1800 °C. It is evident that the prepared samples are porous and non-homogenous. The microstructures are rather similar for all samples. The grey particles are ZrB_2, whereas porosity is black.

Chemical reactions

The reaction sintering of ZrB_2 ceramic sintered by the boron carbide reduction method [15] corresponds to the reaction:

$$2ZrO_2(s) + B_4C(s) + 3C(s) \rightarrow 2ZrB_2(s) + 4CO(g). \quad (1)$$

The standard Gibbs free energy of this reaction is dependent on the temperature according to $\Delta G = 1134 - 0.668T$ (where T is the absolute temperature), according to which the energy is equal to zero under atmospheric pressure at 1425 °C [15]. This reaction is the most effective way to prepare pure ZrB_2 because the only products of the reaction are solid ZrB_2 and carbon monoxide. The following reaction (2) takes place under gradual heating at the temperature 1218 °C:

$$7ZrO_2(s) + 5B_4C(s) \rightarrow 7ZrB_2(s) + 3B_2O_3(g) + 5CO(g). \quad (2)$$

ZrB_2 is formed by reduction of B_4C via reaction (2), and B_2O_3 is produced as an undesirable intermediate product [15]. The reaction (1) begins as soon as the temperature 1425 °C is exceeded.

The preparation of porous ceramic ZrB_2 via reaction (2) and removal of the intermediate B_2O_3 by dissolving has been published [15].

In SPS, the die-punch assembly is not gas-tight. The pressure was applied to compact the powder, and

simultaneously the chamber surrounding the whole SPS setup was evacuated. The SPS technique used for compacting powder was chosen due to the possibility of evacuating the chamber continuously. Thanks to the method the intermediate gaseous CO, released by the reactions (2), is removed from the volume of the consolidated powder and the reaction (1) takes place under lower gas pressure in the chamber.

Exceeding the reaction temperature 1509 °C [15] leads to the reaction of the intermediate B_2O_3 product according to the following formula:

$$ZrO_2(s) + B_2O_3(l) + 5C(s) \rightarrow ZrB_2(s) + 5CO(g). \quad (3)$$

The products of the reaction are ZrB_2 and carbon monoxide. All the reaction temperatures described above depend on the vacuum level, but also on the type of used graphite, as was described in the work [16], which deals with the reaction (3).

The kinetics of the reaction is dependent on the ambient pressure once liquid or gaseous products appear in the reactive synthesis. Reaction (3) is carried out in our case at 1433 °C under atmospheric pressure, but it has been described also at 893 °C under reduced pressure of 10 Pa [16]. Experiments in an inert atmosphere under reduced pressure (the exact value of which was not published) have been reported as well [15, 16]. Only one of the papers [15] mentioned an argon flow rate of 2 l min^{-1} through the sintering chamber. No parameters of the sintering process were described in the papers [15, 16].

The results of the reactive sintering for selected temperatures (1500 °C and 1800 °C, Figures 1 and 2) and factors influencing the production of ZrB_2 by using spark plasma sintering are described below.

The deterioration of the vacuum and the volume increase of the sintering sample at temperatures 450 °C to 500 °C are obvious in Figures 1 and 2. It is described that the melting point of B_2O_3 is between 450 °C and 510 °C depending on the structure of B_2O_3 [16]. Melted B_2O_3 has a high vapour pressure, which leads to its rapid vaporisation at high temperature [16, 18]. B_2O_3 might also react with carbon at temperatures above 700 °C. This statement is validated by our experiments as can be seen in Figures 1 and 2; it is highly probable that B_2O_3 evaporates. Other reactions reported in the literature [16] show that the reaction of intermediate B_2O_3 has a significant role in increasing the yield of ZrB_2 and eliminating the ZrC content [16]. The formation of ZrC starts at 1053 °C and 10 Pa according to the reaction

$$ZrO_2 + 3C \rightarrow ZrC + 2CO. \quad (4)$$

At the same time ZrC reacts with B_2O_3 and carbon at 823 °C and 10 Pa according to the reaction

$$ZrC + B_2O_3 + 2C \rightarrow ZrB_2 + 3CO. \quad (5)$$

It is shown in this experimental study that the intermediate B_2O_3 has a significant influence on the yield and final purity of ZrB_2. If B_2O_3 is completely vaporized at around 500 °C without any donor atoms for boride formation that would have an effect on the yield of reaction 5, B_2O_3 will be present in the reaction mixture. The fact that no donor atoms for boride formation are present in the reaction mixture influences the yield of reaction 3.

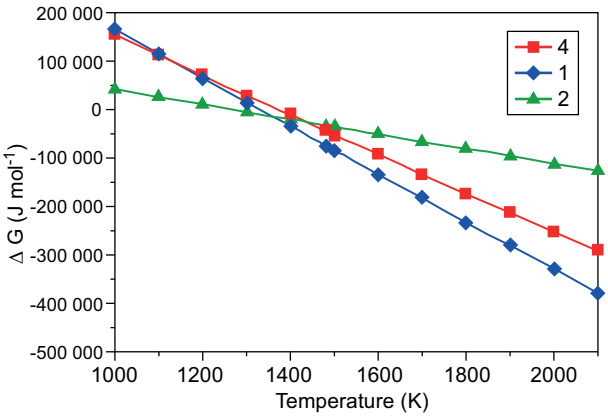

Figure 5. Dependence of the reaction enthalpy on the absolute temperature in Kelvin scale (the numbers in the legend correspond to the reaction formula number in the text above).

From the calculations of the Gibbs reaction enthalpies based on reaction 2 it can be concluded that below 1400 K ΔG_r has a positive value for all reactions and therefore up to that temperature none of the reactions can take place. Above 1400 K all ΔG_r values become negative and all reactions started. Based on the calculations ZrB_2 appears most rapidly (and preferentially) according to reaction 4.

XRD phase analyses

XRD patterns with Rietveld refinements are shown in Figures 6 and 7 for samples prepared at 1500 °C and 1800 °C, respectively. Quantitative phase analysis results for all temperatures are listed in Table 1. The results for samples sintered at 1400 °C show the presence of 52 % ZrB_2, which is a relatively high yield. Actually, according to reaction 2, ZrB_2 is formed at temperatures as low as 1218 °C, and due to the vacuum the reaction temperature is shifted to the right hand side, favoring formation of the products.

Table 1. Results of quantitative XRD phase analysis with Rietveld refinement for samples prepared at temperatures 1400-1800 °C; all values in [wt. %].

Temperature (°C)	ZrO_2	ZrB_2	Graphite	B_4C
1400	32.9	52.1	15.0	-
1500	32.4	54.1	10.4	3.0
1600	30.2	56.8	11.7	1.3
1700	25.2	56.4	13.5	4.9
1800	21.0	63.6	14.6	0.9

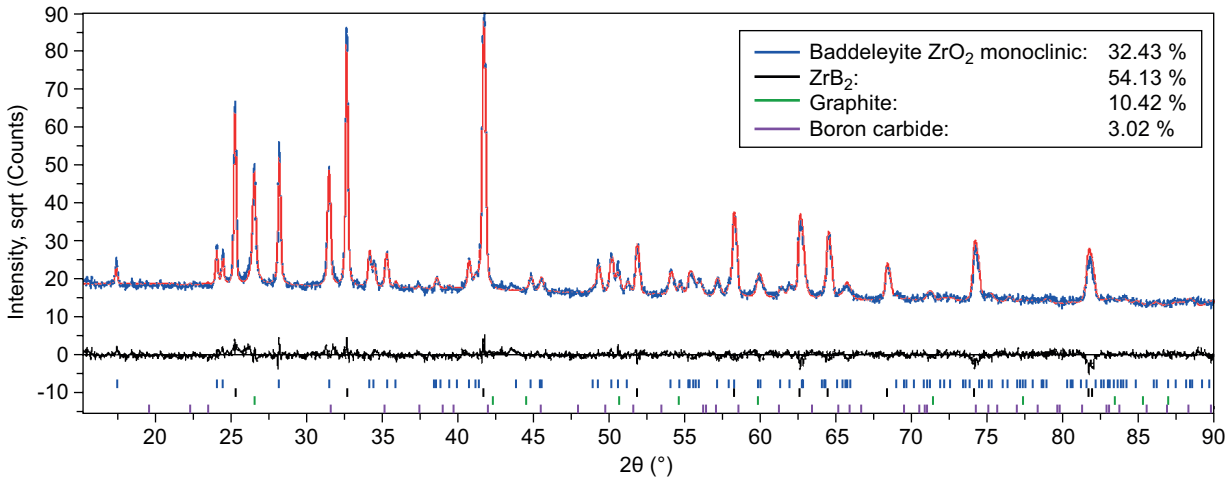

Figure 6. XRD pattern and Rietveld refinement for a sample prepared at 1500 °C.

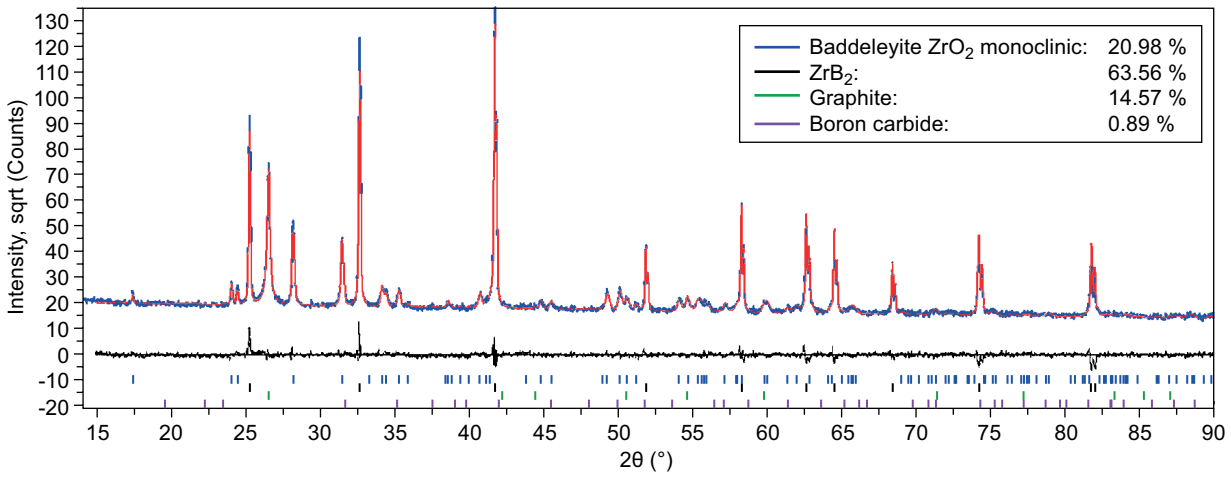

Figure 7. XRD pattern and Rietveld refinement for a sample prepared at 1800 °C.

The yield of the ZrB_2 reaction ranges from 52 % to 64 % for all sintering temperatures. It was published [15, 16] that for achieving a ZrB_2 content of nearly 100 %, 4 mol. % and even 10 mol. % excess of B_4C were used. The samples were heated in a graphite die with a graphite punch. The graphite content of about 10 to 14 % originated from the contamination from the graphite foil inserted between die or punch and the powder feedstock. Yuan et al. [18] investigated reaction sintering with 4 mol. % excess of B_4C sintered at 1250 °C. They achieved almost 100 % of ZrB_2 after 1 hour of sintering. The yield might be increased by combination of B_4C and graphite addition and sintering in an inert atmosphere of argon – at atmospheric or slightly reduced pressure. According to previous knowledge, the use of vacuum to influence kinetics of the reaction proved to be ineffective because of the volatility of B_2O_3, which results in a lower amount of boron (donor atoms) at temperatures above 500 °C.

Porosity

The porosity of the SPS consolidated ZrB_2 samples dropped monotonously from 1.4 % at 1400 °C to 0.3 % at 1800 °C. Simultaneously, the number of pores per mm^2 slightly increased between 1400 °C and 1500 °C, but decreased monotonously to a half of the maximum value for SPS temperatures up to 1800 °C. The content of white zones, Figure 8, increased from 6 % at 1400 °C to 21 % at 1800 °C.

For porosity measurement we applied image analysis of the light optical micrographs. In both light optical and SEM micrographs, there exist a dark (most probably carbon-rich) phase which is difficult to be properly thresholded and separated from porosity, see Figure 8. Besides this "phase" the microstructure contains also white "phase" (probably Zr-rich) and finally some grey particles, the composition of which is difficult to estimate. In general we found a certain increase in the area

fraction of the white zones with temperature at the cost of grey particles. The number of dark zones (porosity plus C-rich component) per mm^2 decreases linearly from 315 at 1500 °C to 130 at 1800 °C. This indicates better sintering or a higher extent of reaction (or a combination of both factors) at higher temperature.

Microhardness

The microhardness was measured by the Vickers indenter attached at optical microscope lens (Hanemann principle). The mean values over the whole microstructure, measured at 1N load, was typically between 3 and 5 GPa, with a high scatter because of irregular microstructure. The microhardness setup enabled us to distinguish between the light grey particles, and the remaining part of the material as a whole. Individual zones were examined at smaller load to fit the indent within a proper object, see Figure 8. The islands with other colours were too fine and did not allow a separate indentation with our lowest available load 250 mN. The hardness of the light grey particles was 9.1 ± 0.5 GPa. The dark grey particles were even harder, up to 20 GPa. The average microhardness value of the whole material was only 3.6 ± 0.7 GPa.

In combination with the data in Table 1 we can conclude that the light grey areas are mainly ZrO_2 (nominal microhardness 12.5 GPa, www.matweb.com), whereas the dark grey particles are ZrB_2 (nominal microhardness 20.9 GPa).

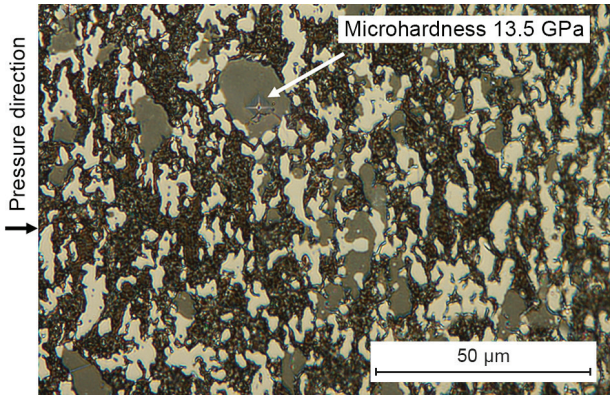

Figure 8. Optical micrograph of a polished section of a sample sintered at 1800 °C with one indent in the particle indicated by arrow (SPS pressure orientation is shown).

CONCLUSIONS

This paper shows how temperature affects the yield of ZrB_2 prepared by SPS reactive sintering. Some reactions are described in this study, especially those where a gas phase is formed and can be detected from the sintering process monitoring, are described in this study. The technological parameters of sintering are discussed in comparison with previously published works, and it was shown that the ZrB_2 phase does not arise from just one reaction, but is accompanied by concurrent and subsequent reactions. At 1500 °C sintering with 15 min of dwell time the reaction yield was only 54 %. The maximum yield of 63 % was achieved at 1800 °C (using the same dwell time). Since a stoichiometric ratio of ZrO_2 and B_4C was used in this work, the yield of the reaction was lower than in other authors' work [18], where more then 10 mol. % excess of B_4C was used.

However, an advantage of our approach is, that despite the presence of carbon (important for boro/carbothermal reduction according to reaction 3) in the starting composition, not ZrC is produced, but only ZrB_2. Due to the fact that the applied pressure of 70 MPa was not high enough for complete porosity elimination, this carbon decreased the entire effectiveness of the ZrB_2 synthesis.

Acknowledgements

The work was supported by the Czech Science Foundation through project number 14-36566G entitled "Multidisciplinary research centre for advanced materials".

REFERENCES

1. Farenholtz W. G.,Hilmans G. E. (2012): Oxidation of ultra-high temperature transition metal diboride ceramics. International Materials Reviews, 54, 61-71. doi:10.1179/174328041 1Y.0000000012
2. Ghaffari S. A., Faghihi-Sani M. A. (2013): Golestani-Fard, F. Ebrahimi, S. Pressureless sintering of $Ta_{0,8}Hf_{0,2}C$ UHTC in presence of $MoSi_2$. Ceramics International, 39, 1985-1989. doi:10.1016/j.ceramint.2012.08.050
3. Ghaffari S. A., Faghihi-Sani M. A., Golestani-Fard F. Mandal H. (2013): Spark plasma sintering of Ta-HfC UHTC via disilicides sintering aids. Journal of the European Ceramic Society, 33, 1479-1484. doi:10.1016/j.jeurceramsoc.2013.01.017
4. Guo S., Kagawa Y., Nishimura T., Chung, D., Yang, J. (2008): Mechanical and physical behavior of spark plasma sintered ZrC-ZrB_2-SiC composites. Journal of the European Ceramic Society, 28, 1279-1285. doi:10.1016/j.jeurceramsoc.2007.08.009
5. Sengupta B., Shekhar S., Kulkarni K. N. (2017): A novel ultra-high strength and low-cost as-cast titanium alloy, Materials Science and Engineering: A, 696, 478-481. doi:10.1016/j.msea.2017.04.106
6. Iida T., Koma M., Ohwa Y., Shudo K., Tanaka M. (2007): Observation of thermal growth of silicide on titanium-deposited silicon surfaces. Surface Science, 601, 18, 4444-4448. doi:10.1016/j.susc.2007.04.214
7. Kubatik T., Jaglova M., Kalabisova E. (2011): Improvement of oxidation resistance of $TiAl_6V_4$ alloy by siliconizing from liquid phase using melts with high silicon content. Journal of Alloys and Compounds, 509, 18, 5493-5499. doi: 10.1016/j.jallcom.2011.02.068

8. Savelli G., Stein S. S., Granger G. B., Faucherand P., Montes L. (2016): Monocrystalline molybdenum silicide based quantum dot superlattices grown by chemical vapor deposition. Superlattices and Microstructures, 97, 341-344. doi: 10.1016/j.spmi.2016.06.042
9. Tan W., Petorak Ch. A., Trice R. W. (2014): Rare-earth modified zirconium diboride high emissivity coatings for hypersonic applications. Journal of the European Ceramic Society, 34, 1–14. doi: 10.1016/j.jeurceramsoc.2013.07.016
10. Guo S., Kagawa Y., Nishimura T. (2008): Elastic properties of spark plasma sintered (SPSed) ZrB_2–ZrC–SiC composites. Ceramics International, 34, 1811–1817. doi: 10.1016/j.ceramint.2007.06.010
11. Akin I., Hotta M., Sahin F. C., Yucel O. (2009): Microstructure and densification of ZrB_2–SiC composites prepared by spark plasma sintering. Journal of the European Ceramic Society, 29, 2379–2385. doi: 10.1016/j.jeurceramsoc.2009.01.011
12. Grigoriev O. N., Galanov B. A., Lavrenko V. A, Panasyuk A. D, Ivanov S. M, Koroteev A. V., Nickel K. G. (2010): Oxidation of ZrB_2–SiC–$ZrSi_2$ ceramics in oxygen. Journal of the European Ceramic Society, 30, 2397–2405. doi: 10.1016/j.jeurceramsoc.2010.03.016
13. Zou J., Zhang G. J., Hu Ch. F., Nishimura T., Sakka Y., Tanaka H., Vleugels J., Biest O. V. (2012): High-temperature bending strength, internal friction and stiffness of ZrB_2-20 vol % SiC ceramics. Journal of the European Ceramic Society, 32, 2519–2527. doi: 10.1016/j.jeurceramsoc.2012.01.035
14. Han J., Hu P., Zhang X., Meng S., Han W. (2008): Oxidation-resistant ZrB_2-SiC composites at 2200 °C. Composites Science and Technology, 68, 799–806. doi:10.1016/j.compscitech.2007.08.017
15. Jung E. Y., Kim J. H., Jung S. H., Choi S. C. (2012): Synthesis of ZrB_2 powders by carbothermal and borothermal reduction. Journal of Alloys and Compounds, 538, 164–168. doi:10.1016/j.jallcom.2012.05.076
16. Qiu H. Y., Guo W. M., Zou J., Zhang G. J (2012): ZrB_2 powders prepared by boro/carbothermal reduction of ZrO_2: The effect of carbon source and reaction atmosphere. Powder Technology, 217, 462–466. doi:10.1016/j.powtec.2011.11.002
17. Yuan H., Li J., Shen Q., Zhang L. (2012): In situ synthesis and sintering of ZrB_2 porous ceramics by the spark plasma sintering–reactive synthesis (SPS–RS) method. International Journal of Refractory Metals and Hard Materials, 34, 3–7. doi:10.1016/j.ijrmhm.2012.01.007
18. Yuan H., Li J., Shen Q., Zhang L. (2013): Preparation and thermal conductivity characterization of ZrB_2 porous ceramics fabricated by spark plasma sintering. International Journal of Refractory Metals and Hard Materials, 36, 225–231. doi:10.1016/j.ijrmhm.2012.09.003